doi:10.2533/chimia.2024.869 Chimia 78 (2024) 869–877

Intermetallic Materials for High-Capacity Hydrogen Storage Systems

Nazar Pavlyuk[a], Vasyl Kordan[a], Grygoriy Dmytriv[a,*], Maksym Yarema[b,*], and Volodymyr Pavlyuk[a,c,*]

Abstract: In this article, we provide an overview of hydrogen storage materials, taking our previous results as examples. Towards the end of the paper, we present a case study in order to highlight the effects of substitutional alloying, compositional additives, and nanostructuring on the hydrogen sorption properties of magnesium-based intermetallics. Specifically, partial substitution of Mg by Li and *d*-elements by *p*-elements leads to structural changes, inducing disorder and the formation of high-entropy alloys. Our approach showcases the methodology to enhance the H_2-capacity and to provide a positive boost to the H_2-storage performance, including lower temperatures of H_2 desorption, better thermodynamics and kinetics, lower temperatures of hydrogen uptake/release for Metal-Hydride Hydrogen Storage (MHHS) systems and higher capacity of anodes for Metal-Hydride batteries (MHB) together with lower prices of raw materials.

Keywords: Batteries · Hydrogen storage systems · Intermetallics · Nanomaterials

Dr. Nazar Pavlyuk is a researcher at the Department of Inorganic Chemistry, Ivan Franko National University of Lviv, Ukraine. His scientific work covers topics of magnesium-based intermetallics, high-entropy alloys and metal-hydrides. He is experienced in single-crystal/powder XRD structural investigations and the creation of new materials for hydrogen storage systems and battery applications. In 2023 he successfully defended his PhD thesis. He is also a co-founder and CEO of the startup 'Lviv Hydrogen', dealing with hydrogen storage using our metal-hydride material.

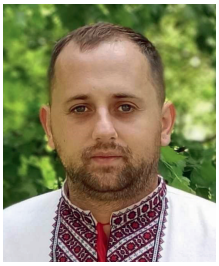

Dr. Vasyl Kordan has more than 10 years of scientific experience. He earned his Master in Chemistry in 2014 and PhD in 2018 at the Inorganic Chemistry department, Ivan Franko National University of Lviv. He is the co-author of more than 50 scientific publications on crystal structures, hydrogen sorption electrochemical and properties of intermetallic compounds. Now he is a Senior Research Fellow at the Department of Inorganic Chemistry, Ivan Franko National University of Lviv.

Prof. Dr. Grygoriy Dmytriv holds a doctorate in inorganic chemistry from Ivan Franko National University of Lviv. Currently, he is a dean of the Faculty of Chemistry at this University. His research focuses on lithium and magnesium alloys for application in battery materials and hydrogen storage materials. His work has been recognized by several awards, including scholarships for work at Jagiellonian University and Technical University Darmstadt. He was the leader of two international grants from the SIMONS foundation and head of the organizing committee of international conferences. He was elected as Honorary Ambassador of Lviv for wide international scientific cooperation.

Prof. Dr. Volodymyr Pavlyuk is a distinguished professor of the Ivan Franko Lviv National University, laureate of the State Prize of Ukraine in Science and Technology (nominated and awarded by President of Ukraine, 2008). His scientific activity is also closely connected with the Jan Długosz University in Częstochowa, Poland. His scientific work focuses on the synthesis of new intermetallic compounds, phase diagram investigations, crystal structure determination, crystal chemistry, as well as physical and electrochemical property analyses of alloys. Materials based on these alloys are of great importance for energy technology with optimized Li-ion, Mg-ion, and metal-hydride batteries.

Prof. Dr. Maksym Yarema is head of Chemistry and Materials Design Group at the Institute of Electronics, ETH Zurich. His research focus is on the interface between chemistry and device science. He has authored over 80 publications about various aspects of nanoscience, optoelectronics, energy storage, and memory devices. He is a recipient of several awards and fellowships, such as ERC Starting Grant, SNSF Ambizione Fellowship, and Marie Curie Postdoc grant. His academic commitments include organization of IUPAC and MATSUS conferences, editorial collaborations with ACS and Frontiers, development of international teaching programme, and involvement in several Advisory Boards and Selection Committees.

*Correspondence: Prof. Dr. G. Dmytriv, E-mail: grygoriy.dmytriv@lnu.edu.ua; Prof. Dr. M. Yarema, E-mail: yaremam@ethz.ch; Prof. Dr. V. Pavlyuk, E-mail: v.pavlyuk@ujd.edu.pl.
[a]Department of Inorganic Chemistry, Ivan Franko National University of Lviv, Kyryla i Mefodiya St. 6, 79005 Lviv, Ukraine; [b]Chemistry and Materials Design Group, ETH Zurich, Gloriastrasse 35, CH-8092 Zurich, Switzerland; [c]Institute of Chemistry, Jan Długosz University, al. Armii Krajowej 13/15, 42-200 Częstochowa, Poland.

1. Introduction

Hydrogen (H_2) storage is important for sustainable technologies of the future, such as clean energy source, environmentally friendly automotive industry or metal hydride batteries. The main requirements for modern energy-source and hydrogen storage materials in automotive applications are high gravimetric density (above 4 wt.% gravimetric capacity of hydrogen), absorption/desorption of hydrogen at moderate temperatures and pressures, relatively low cost of the material, and environmental safety.[1] Conventional metal hydrides, such as $LaNi_5$ and its substitutional derivatives, titanium and zirconium alloys that are commonly used as hydrogen storage systems, have the capacity of nearly 1.5 wt.% and thus cannot satisfy current needs. New materials developed on the basis of light metals such as Mg and Li are promising candidates of being potential light-weight hydrogen storage materials.[2] Super-lightweight intermetallics from the Mg-Li-Si ternary system are promising hydrogen storage materials that absorb the highest amount of hydrogen at 8.8 wt.%.[3] For example, we have synthesized and investigated $Li_{12+x}Mg_{3-x}Si_4$ compounds, which absorbs the highest amount of hydrogen among all known intermetallic compounds (Fig. 1), with a derivative $Li_{12+x}Mg_{3-x}Si_{4-y}Sn_y$ phase absorbing stunning 8.9 wt.% of H.[4] This number can be enhanced even further using carbonaceous dopants.[5] Specifically, using carbon nanotubes for $Li_{12+x}Mg_{3-x}Si_{4-y}Sn_y$, hydrogen weight percentage can be enhanced up to 9.2 wt.%.[4] Concerning hydrogenation properties, the main issue of magnesium hydride and magnesium-based alloy hydrides is the formation of stable hydrides with high temperatures and pressures of hydrogenation and dehydrogenation.

In next sections, we review main classes of H_2-storage intermetallic materials.

1.1 *Rare-Earth Metal Hydrides*

Intermetallic compounds like $LaNi_5$ and $SmCo_5$ represent a class of intermetallic materials with notable potential in hydrogen storage applications. These compounds exhibit advantageous properties such as good reversibility and substantial hydrogen storage capacity, maximizing up to 2 wt.% of H.[6] Bimetallic Laves phases like $TiMn_2$ and $ZrFe_2$ comprise a second generation of H_2 storage materials.[7] Due to their specific crystal structure, Laves phase compounds demonstrate stability in hydride formation, contributing to their consideration in the quest for sustainable H_2 storage materials.

1.2 *Ternary Laves Phases*

Ternary Mg-T-M intermetallics (where T is Mn, Fe, Co, Ni and M is Al, Ga, Sn, Sb) are interesting systems for materials discovery for H_2 storage applications. Investigating these materials, we seek ternary phases that have many tetrahedral and octahedral voids in its crystal structure. As it is known, hydrogen absorbed into the volume of material is placed in these voids. One of the most promising candidate phases are so called Laves phases that do occur often with these materials and show promising hydrogen storage properties.

There is a number of Laves phases that we have tested for the practical hydrogenation properties. The most promising one is $MgNi_{1+x}Ga_{1-x}$ ($x = 0.25$), which absorbs 2.2 wt. % of H and releases 1.9 wt. %.[8] Moreover this phase is at least cyclically stable for 5 cycles (Fig. 2).

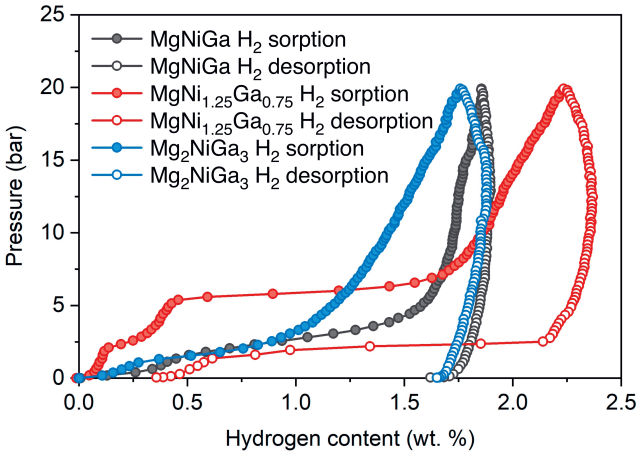

Fig. 2. The P-C isotherms of hydrogen absorption/desorption process for $MgNi_{1.25}Ga_{0.75}$, MgNiGa, and Mg_2NiGa_3 (or $MgNi_{0.50}Ga_{1.50}$) Laves phases at the temperature of 300 °C.[8]

The second promising candidate phases are $MgNi_2Al$ and $MgCo_2Al$.[9] The maximum weight percentage of hydrogen is slightly lower: 1.34% for $MgCo_2Al$ and 1.38% for $MgNi_2Al$, rendering the compositions of the respective hydrides to $MgCo_2AlH_{2.3}$ and $MgNi_2AlH_{2.4}$. The key advantage, however, is that both intermetallic hydrides release hydrogen fully (H_2 content goes down to 0 wt.%), thus $MgNi_2Al$ and $MgCo_2Al$ phases are both applicable for a practical use (Fig. 3).

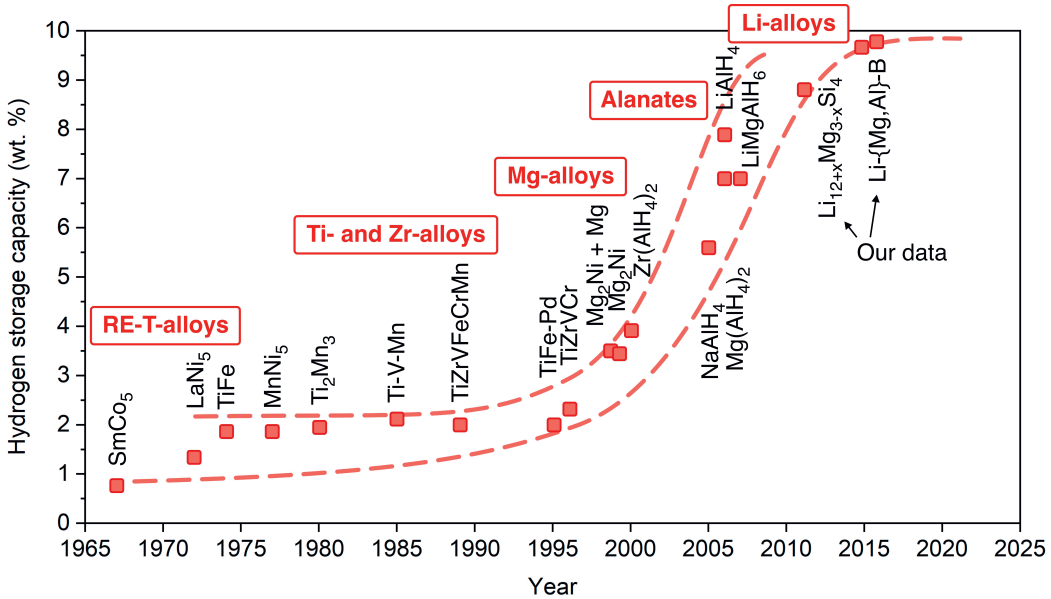

Fig. 1. Hydrogen storage capacity of intermetallics.[3]

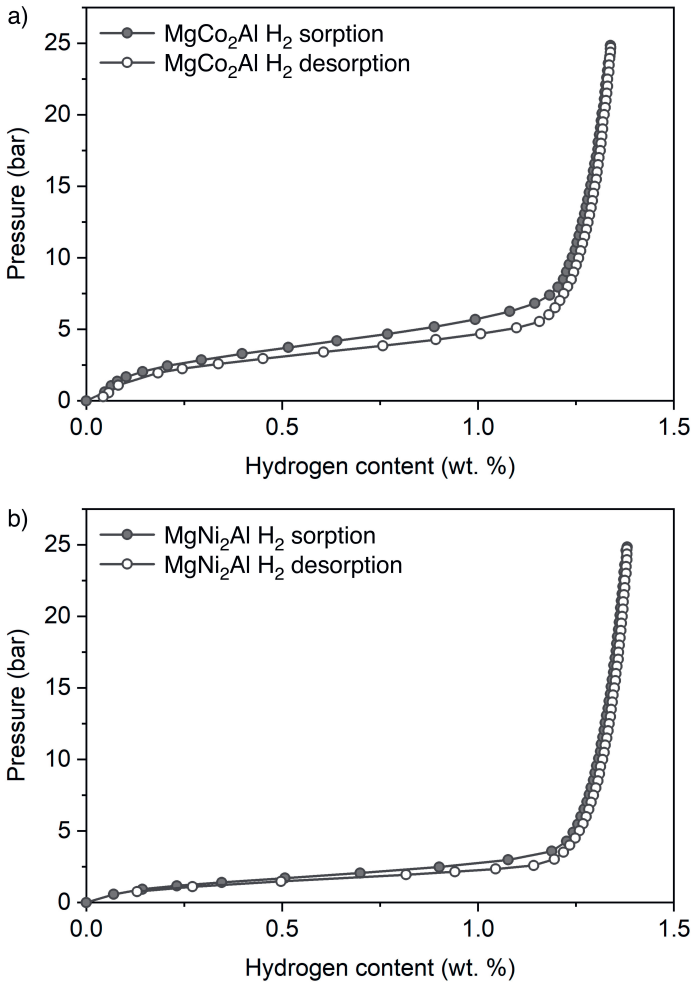

Fig. 3. The P-C isotherms of hydrogen absorption/desorption process for $MgCo_2Al$ and $MgNi_2Al$ intermetallic compounds. These measurements were carried out at T = 80 °C.[9]

1.3 *Lightweight Intermetallic Compounds*

Compared to traditional intermetallic materials, alloys based on Mg, Li, and Al hold key benefits for H_2 storage applications, such as light weight. Besides, Mg-based alloys offer improved mechanical properties and enhanced corrosion resistance, rendering them unique for a range of applications in nuclear, aviation, aerospace, automotive and metallurgical industries. For example, Mg-Li alloys were firstly produced in the 1960s by NASA for aerospace purposes.[10] Mg-Li-based intermetallics belong to the so-called superlight alloys. Their density depends on the composition and can be as low as 1.05-1.50 g/cm^3. To compare, the Mg-Li alloy castings are up to 30% lighter than castings from aluminum alloys, and 50-70% lighter than iron-based castings.[10–13]

Ternary and quaternary Mg-based and Mg-Li-based alloys are particularly interesting due to their ability to absorb large amounts of H_2. We have previously studied the Mg-Li-M and Mg-T-M intermetallic systems (where T is Mn, Fe, Co, Ni and M is Al, Ga, Sn, Sb) in extensive details. For example, we have prepared new $Mg_{76}Li_{12}Al_{12}H_x$ hydrides using several synthetic methods, such as gas phase hydrogenation, thermal and electrochemical synthesis.[14] Interestingly, two hydride phases are formed from the interaction of $Mg_{76}Li_{12}Al_{12}$ alloy with hydrogen. In the first stage, we observe the insertion of up to 3.2 wt.% H into the structure of the initial hexagonal phase This reversible hydride has a composition of $Mg_{76}Li_{12}Al_{12}H_x$ (0<x<74) and a hexagonal crystal structure (P-6m2, a = 3.1485(1), c = 5.1111(2) Å) in which hydrogen atoms are inserted into octahedral voids. During the second stage of hydrogenation, a new $Mg_{76}Al_{12}Li_{12}H_x$ (74<x<200) hydride phase with higher hydrogen content up to 8.2 wt.% H is formed. This hydride has an orthorhombic structure (*Cmmm*, a = 6.8198(3), b = 6.8543(3), c = 3.3609(1) Å) in which hydrogen atoms have coplanar triangle coordination (Fig. 4). This $Mg_{76}Al_{12}Li_{12}H_x$ hydride is lightweight while also having a higher hydrogen content compared to binary MgH_2 hydride (7.6 wt.% H).

We further studied the electrochemical hydrogenation of Mg-based solid solution phase with $Mg_{76}Li_{12}Al_{12}$ composition, using various electrochemical methods and the structure of obtained hydrides. As for the latter, the structure of $Mg_{76}Li_{12}Al_{12}H_x$ ($0 < x < 74$) hydride appears to be strongly disordered, as evidenced by the presence of statistical mixtures in atomic sites, therefore, in

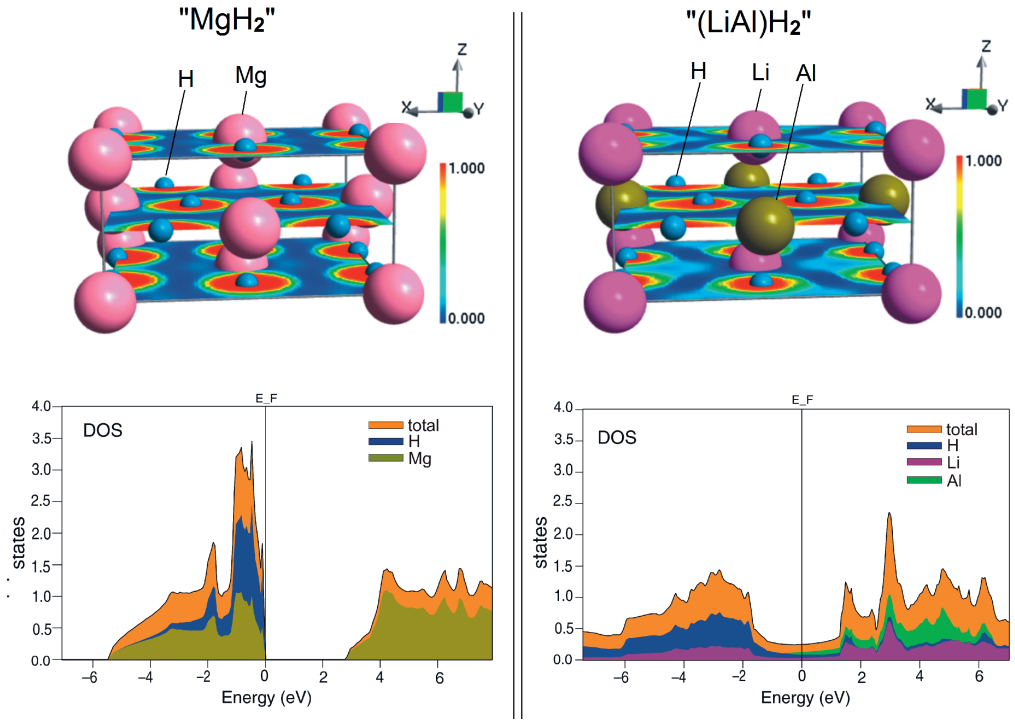

Fig. 4. The electron localization function (ELF) mapping and the total and partial distribution of states (DOS) for the MgH_2 and $(LiAl)H_2$ subcells.[15]

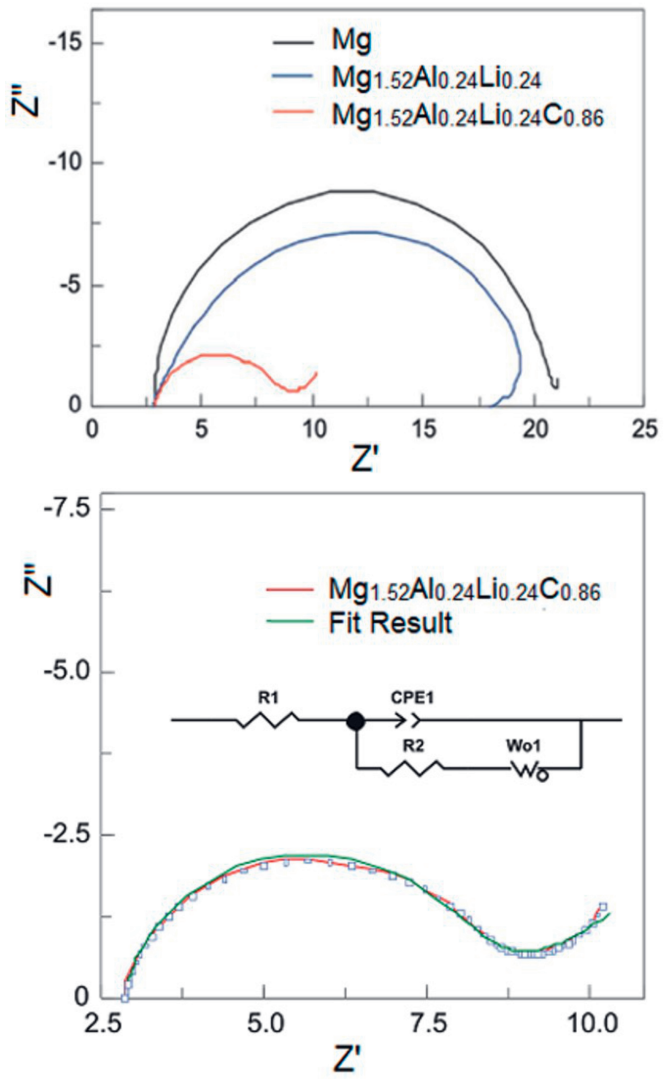

Fig. 5. EIS data for the $Mg_{1.52}Li_{0.24}Al_{0.24}C_{0.86}$ electrode in 6M KOH solution.[16]

the average structure, two subcells ('MgH_2' and '$(LiAl)H_2$') with a fraction ratio of subcells as 7:1 respectively can be selected. We then perform calculations of the electronic structure for both subcells.[15] A higher electron localization function within the crystal space is observed around the H atoms in both structure models (Fig. 4). The minimum electron localization function (blue region) was observed around the Mg and Li/Al atoms. These significant differences in the values of the functions of electronic localization indicate the presence of ionic interactions between atoms of hydrogen and metals.

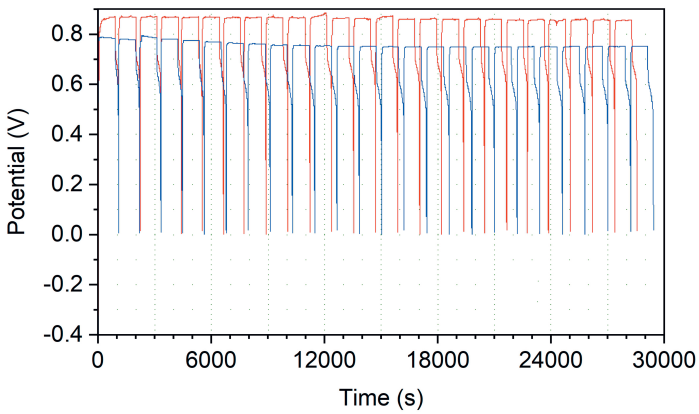

Fig. 6. Galvanostatic charge/discharge (i_{charg} = 2 mA cm^{-2}, i_{disch}= 1 mA cm^{-2}) cycles for Mg (red) and $Mg_{76}Li_{12}Al_{12}$ electrodes (blue).[16]

The ability of magnesium alloys to be electrochemically hydrogenated opens another exciting avenue of research: metal hydride batteries (MHB). Our electrochemical investigation of electrodes prepared from the quaternary $Mg_{1.52}Li_{0.24}Al_{0.24}C_{0.86}$ and ternary $Mg_{1.52}Li_{0.24}Al_{0.24}$ alloys shows more effective passivation of the carbide electrode in strong alkaline solutions with respect to the Mg reference.[16] Impedance measurements by EIS show a gradual evolution of the impedance spectra with the composition of electrodes (pure Mg, ternary phase, and quaternary compound). As shown in Fig. 5, the diameters of the semicircles observed for the $Mg_{1.52}Li_{0.24}Al_{0.24}C_{0.86}$ alloy electrode are smaller than those of the Mg metal and $Mg_{76}Li_{12}Al_{12}$ electrodes, which demonstrates that the charge-transfer reaction is facilitated for the carbide electrode.

Reversible hydrogen storage capacity of these compounds reached 3.2 wt.% H, corresponding to 865 mAhg^{-1}. After final charging/discharging cycles, the initial $Mg_{76}Li_{12}Al_{12}$ solid solution phase was recovered, indicating that the electrochemical reactions are reversible (Fig. 6).

As can be seen in Fig. 6, for subsequent cycles, the plateau region for $Mg_{76}Li_{12}Al_{12}$ alloy electrode increases, meaning that discharge times are getting longer, and thus at the cycling, the capacity of the alloy electrode increases compared to that of the Mg metal electrode.

1.4 *Composite Additives*

Carbon nanotube (CNT) additives can be blended with intermetallic phases to improve their hydrogen absorption/desorption processes. In our previous research paper, we studied a synergy of Li_xZnO-CNT and La_2O_3-CNT composite additives (CA) on $Li_{12-x}Mg_{3-x}Si_{4-y}Sn_y$ intermetallics (Fig. 7). The effect of the addition of composite additives on the improvement of hydrogen sorption kinetics of the intermetallic phase is due to the following factors: (i) the addition of a CA increases the stability of Li-containing alloys; (ii) CA provides diffusion pathways to most of the grains inside the material, where the dissociation of H_2 molecules into H atoms takes place; (iii) CA surface has a relatively higher reactivity to H_2 dissociation.[8]

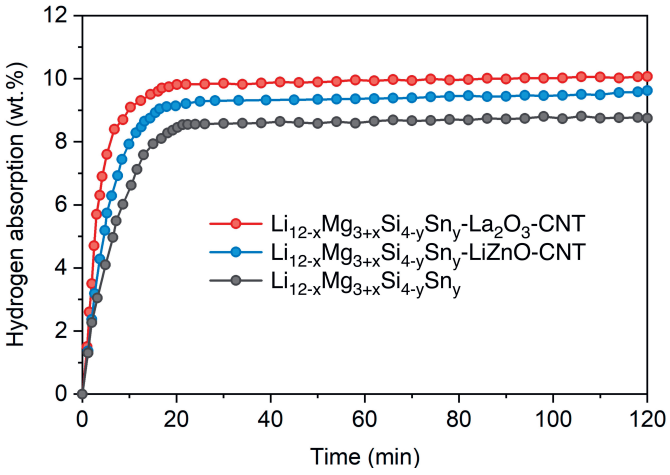

Fig. 7. Hydrogen absorption curves of samples at 380 °C after activation.[8]

The enthalpy of hydrogen desorption for samples $Li_{12-x}Mg_{3+x}Si_{4-y}Sn_y$, $Li_{12-x}Mg_{3+x}Si_{4-y}Sn_y$-$La_2O_3$-CNT and $Li_{12-x}Mg_{3+x}Si_{4-y}Sn_y$-LiZnO-CNT (Fig. 8) are lower than for the $Li_{12}Mg_3Si_4$-H (99 kJ/mol) and the ability to hydrogen uptake is higher, which clearly indicates that the substitution of Si by Sn and

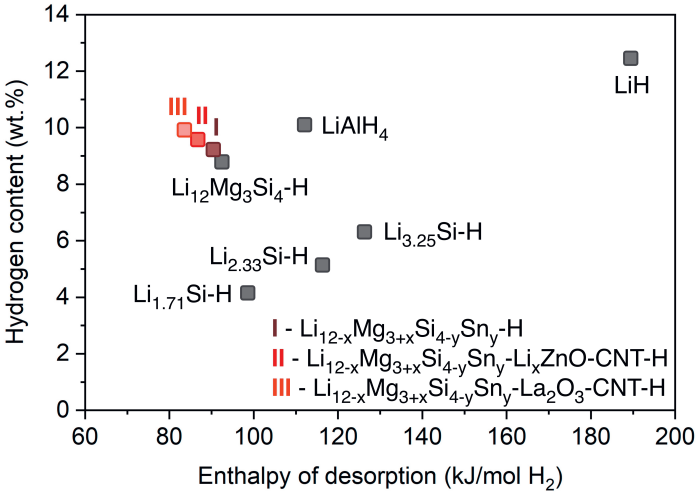

Fig. 8. Hydrogen content and enthalpy of desorption of some lithium-containing hydrides. Note the beneficial effects of composite additives, such as higher H_2 content and lower enthalpy of desorption.[4]

doping by La_2O_3-CNT and LiZnO-CNT composites has a positive effect on the processes of hydrogenation and dehydrogenation.

2. Case Study for Quaternary Intermetallics

2.1 *Disorder in Intermetallic Hydrides*

We present one of the approaches for the creation of hydride active materials using the example of Mg-Li-T-M systems (where T is Mn, Fe, Co, Ni, and M is Al, Ga, Sn, Sb). Alloys of these systems can be used in metal-hydride hydrogen storage systems (MHHSS) and metal-hydride batteries (MHB). We select three series of intermetallic compounds as the starting phases for synthesis, and afterward we create composition series, tuning the amounts of constituent metals: $Mg_{2-x}Li_xT_{1-y}M_y$, $Mg_{1-x}Li_xT_{1-y}M_y$, and $Mg_{1-x}Li_xT_{2-y}M_y$. The partial substitution of Mg atoms by Li and transition metals by p-elements results in the formation of alloys with maximally disordered intermetallic phases. These partial substitutions by Li and by p-elements can also lead to changes in structure and an increase in H_2 capacity. As a result of the substitution of Mg by Li and T by M and their hydrogenation, the new disordered high entropy intermetallic phases (HEIP) were formed and studied (Fig. 9). The concept of high entropy alloys introduces the development of advanced materials with unique properties that cannot be achieved by conventional alloys based on only one dominant element. High entropy alloys can be used to create materials with high thermal and corrosion stability, oxidation resistance, with improved mechanical and electrochemical properties.

2.2 *Modification with Composite Additive*

The next important step is the modification of the electrodes by composite additives (CA), such as carbon nanotubes (CNT) catalysts, in order to increase the capacity of H_2 storage material and improve their cyclic stability. CNTs are effective composite additives both for MHHS systems and MHB usage. This modification has been performed for $Mg_{2-x}Li_xT_{1-y}M_y$, $Mg_{1-x}Li_xT_{1-y}M_y$, and $Mg_{1-x}Li_xT_{2-y}M_y$ ($0<x,y<0.5$) phases. We added different amounts of CNT, namely 5 wt.%, 10 wt.% and 15 wt.% to alloys with subsequent mixing, pressing and sintering (Fig. 10).

2.3 *Characterization of Materials*

Finally, we carried out the hydrogenation experiments and characterization, quantifying the H_2 capacity, rate, and longevity. Our electrochemical studies have shown that the optimal amount of CNT is 10 wt.%. Modification of alloys with carbon nanotubes catalysts allowed to significantly increase the discharge capacity of NiMH batteries from 150 $mAhg^{-1}$ up to 165 $mAhg^{-1}$. The study of cyclic stability shows that for catalytically modified electrodes after 50 cycles of charge-discharge capacity decreases by no more than 10% (Fig. 11).

2.4 *Mechanistic Interpretation*

CNT additives act as catalyst and the electrochemical hydrogenation for generalized MgTM phase can be written as:

Non-catalyzed reaction

$$MgTM + nH^+ + ne^- \rightleftarrows [MgTM \cdots nH] \rightleftarrows MgTMH_n \quad (1)$$

Catalyzed reaction

$$MgTM + CNT + nH^+ + ne^- \rightleftarrows MgTM + [CNT \cdots nH] \rightleftarrows [MgTM \cdots H \cdots CNT] \rightleftarrows MgTMH_n + CNT \quad (2)$$

The pathway for the catalyzed reaction has two steps (Fig. 12). However, the energetic barriers for both steps are much lower than for direct uncatalyzed process (Eqn. I). The overall lower activation energy can explain why catalyzed reaction (Eqn. II) is faster. Provided schematics (Fig. 12) suggests to employ alloying or doping strategies to improve performance of selected materials for use as Metal Hydride Hydrogen Storage and anodes in Metal-Hydride batteries.

The data from Sieverts-type volumetric apparatus and thermal analysis methods were used to calculate the activation energy for $MgTMH_z$ (T = Ni) hydride decomposition by applying the Kissinger equation.[17] The dehydrogenation activation energy of the MgTM-CNT modified sample was 87.9 kJ/mol (catalyzed reaction), which was much lower than that of the MgTM unmodified alloy (125.6 kJ/mol) for uncatalyzed reaction. The obtained value of the activation energy for MgTM is of the same order as those determined and given in the literature for $Mg_2Ni_{0.9}Co_{0.1}$ alloy (94.7 kJ/mol).[18]

3. Outlook

3.1 *Aging of H_2 Storage Materials*

The amorphization problem in hydrogen storage materials poses a significant challenge in the development of efficient and durable hydrogen storage systems. Many hydrogen storage materials, including metal hydrides and complex hydrides, undergo structural changes during the absorption and desorption of hydrogen, commonly known as cycling. While these changes are often reversible in crystalline materials, some materials experience irreversible transformations leading to amorphization – a state characterized by the loss of long-range order in the atomic arrangement.

Amorphization brings about several challenges for hydrogen storage applications. One critical consequence is the reduction in hydrogen storage capacity.[19] As a result of structural order loss, the materials store and release less hydrogen, negatively impacting the overall performance of the hydrogen storage system. Furthermore, the lack of a well-defined crystalline structure can slow down the rates of hydrogen absorption and desorption, affecting the responsiveness of the material to dynamic hydrogen-related processes.

Efforts to address the amorphization problem are concentrated on designing materials with improved resistance to structural degradation. Specifically, the strategy of nanostructuring may enhance the reversibility and stability of hydrogen storage materials. Therefore, intermetallic nanocrystals appear as a

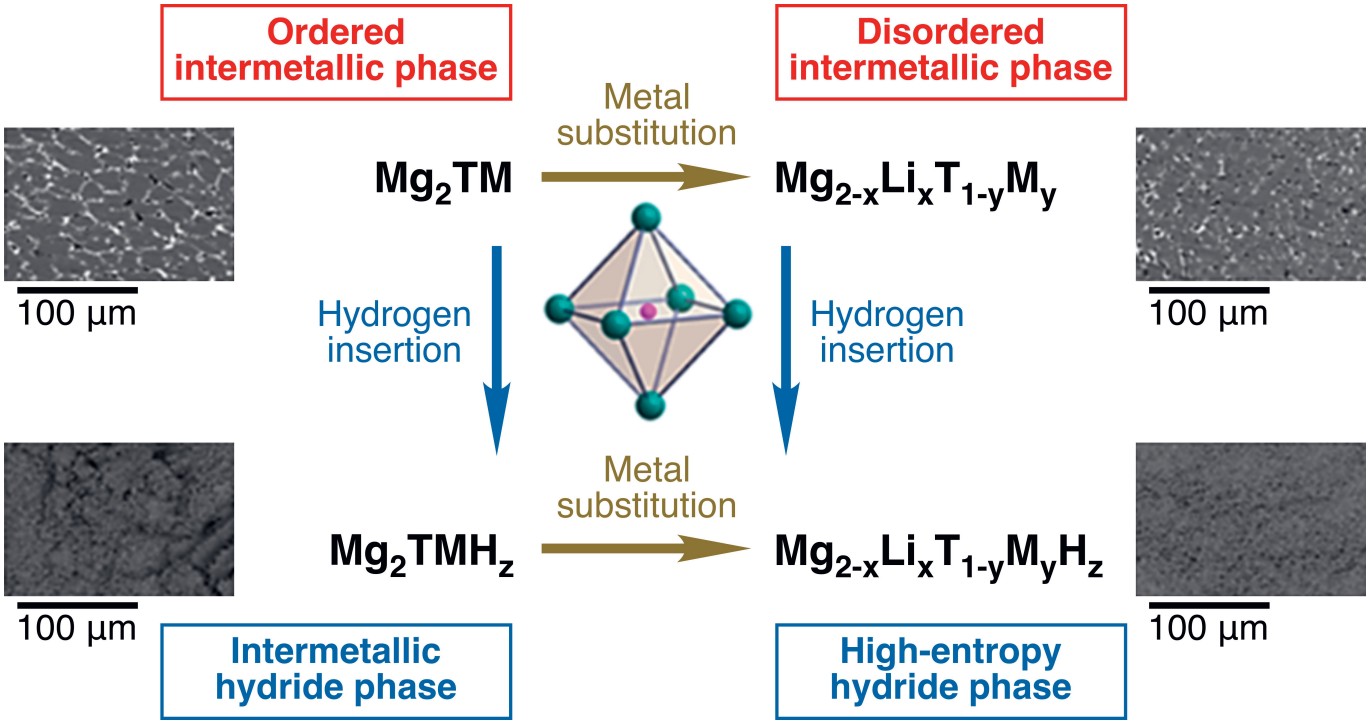

Fig. 9. Schematics for the formation of disordered alloys and their high entropy hydride phases. The center of the figure shows an octahedral site into which the hydrogen atom is inserted. SEM micrographs illustrate grain size reduction for high entropy phases.

promising solution to mitigate the amorphization of hydrogen storage materials. Their nanoscale size reduces diffusion lengths, facilitating more controlled hydrogen absorption and desorption. Additionally, the dynamic lattice of nanocrystals, inherent to their small dimensions, enhances their resilience against cycling-induced stress. This dynamic behavior allows nanocrystals to better accommodate the strains associated with repeated hydrogen cycling, reducing the likelihood of irreversible amorphization.

3.2 *Intermetallic Nanocrystals for H_2 Storage*

In addition to tackling the aging of H_2 storage materials, intermetallic nanocrystals confer several other advantages that hold promise to enhance H_2 storage properties.[20] One of the primary benefits lies in the vastly increased surface area. Due to their small size, nanocrystals boast an exceptional surface-to-volume ratio, providing an extensive array of active sites for the adsorption and desorption of hydrogen molecules. Furthermore, intermetallic nanocrystals demonstrate improved kinetics in hydrogen-related processes. The small size facilitates faster diffusion of hydrogen atoms within the material, leading to accelerated rates of hydrogen uptake and release. Finally, nanocrystals exhibit size-dependent thermodynamics, which can be utilized for hydrogen storage capabilities in creating favorable thermodynamic conditions for hydrogen adsorption and desorption, further optimizing the overall efficiency of the storage process.

Despite their potential, intermetallic nanocrystals are rarely studied for H_2 storage applications. One of the reasons is the lack of reliable synthetic approaches for intermetallic nanocrystals. Recently, we provided a possible solution, discovering a synthesis which unlocks up to a 1000 of intermetallic phases in the form of high-quality colloidal nanocrystals.[21] The approach is based on amalgamation alloying and works for any combination of liquid and solid metals (Fig. 13). Briefly, liquid metal (LM) is dispatched to the surface of solid metal seeds *via* the thermolysis of LM amide salt. The LM patches undergo a fast amalgamation alloying at the nanoscale, forming homogeneous and phase-pure intermetallic nanocrystals. The nanoscale amalgamation reaction allows the synthesis of many phases within the same diagram. For example, γ-brass Pd_3Zn_{10}, cubic PdZn, and *fcc*-type Zn-doped Pd nanocrystals can be prepared with excellent phase purity by simply tuning the amount of Zn amide introduced in the reaction

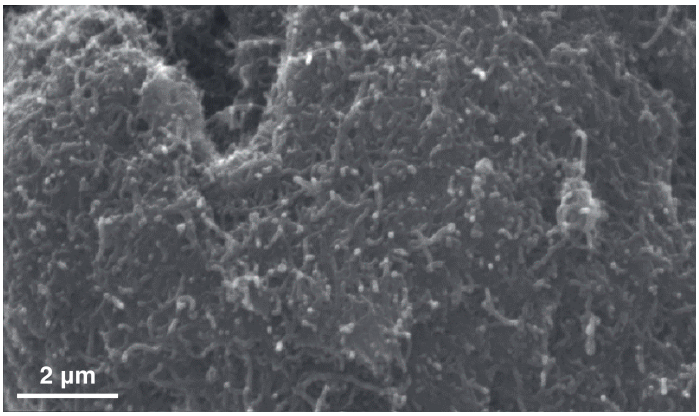

Fig. 10. SEM image for quaternary alloy modified by CNT.

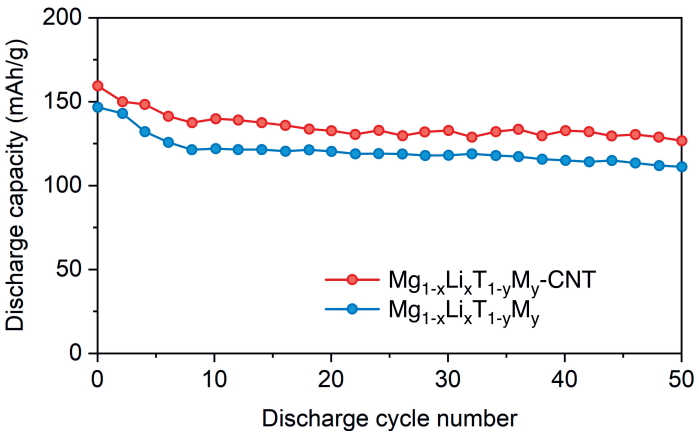

Fig. 11. Specific capacities *vs.* cycle number of the tested alloy with and without modification by CNT.

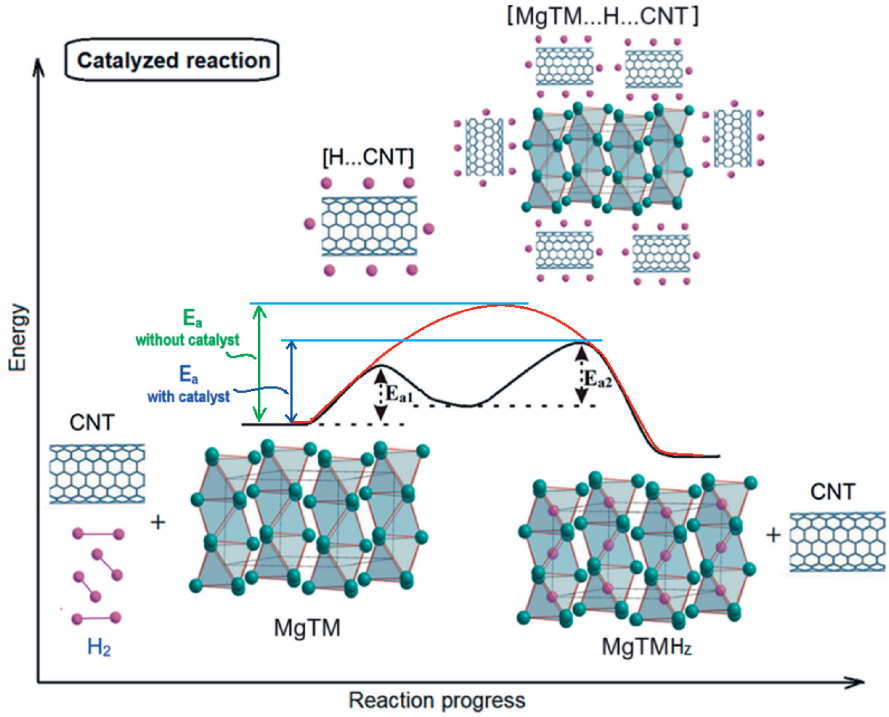

Fig. 12. A schematic representation of the reaction profile of a reaction with a CNT catalyst.

mixture.[22] Furthermore, the size of intermetallic nanocrystals remains controlled solely by the size of initial seeds.[21] Taken together, the nanoscale amalgamation reaction offers exciting opportunities for nanoscale H_2 storage materials, which can now be prepared with accurate size and composition control.

4. Experimental Section

4.1 *Synthesis of the Materials*

Bulk intermetallic alloys were prepared by classical solid-state methods, such as induction and arc melting. The starting materials for the preparation of the alloys were pure metals. All preparation steps were performed in a glove box under a dried argon atmosphere. The melting of metals was carried out within sealed tantalum crucibles in an induction furnace at 700–1100 ºC. After 10 min, the samples were rapidly cooled down to room temperature by removing the crucible from the furnace. The overall composition of the alloys was chosen with respect to the nominal composition of the known or expected compounds. Deviations from these nominal compositions were selected to probe the homogeneity ranges of solid solutions of the included phases. Afterwards, the bulk intermetallic alloys were powderized by the high energy ball milling method.

Annealing was done for the samples prepared by the classical solid-state methods. Annealing of the prepared alloys was already performed in tantalum crucibles. Furnaces with automatic temperature control were used for the homogenizing and annealing of the alloys. For all systems the temperature of annealing was adjusted individually, depending on the composition of alloys. The time of annealing was adjusted for each system, and it can be up to 400 hours.

The compositional series were carried out starting with different ratios of metals for the classical solid-state synthesis. Alternatively, electrochemical lithiation and delithiation as the means of nanoscale colloidal amalgamation method can be explored.

4.2 *Phase Analysis of Samples*

X-ray powder diffraction (XRD) was applied as the method of choice for phase analysis and crystal structure refinements. Intensity data was collected in STOE STADI P (MoKα1 radiation) and RIGAKU Miniflex D-600 (CuKα1 radiation)

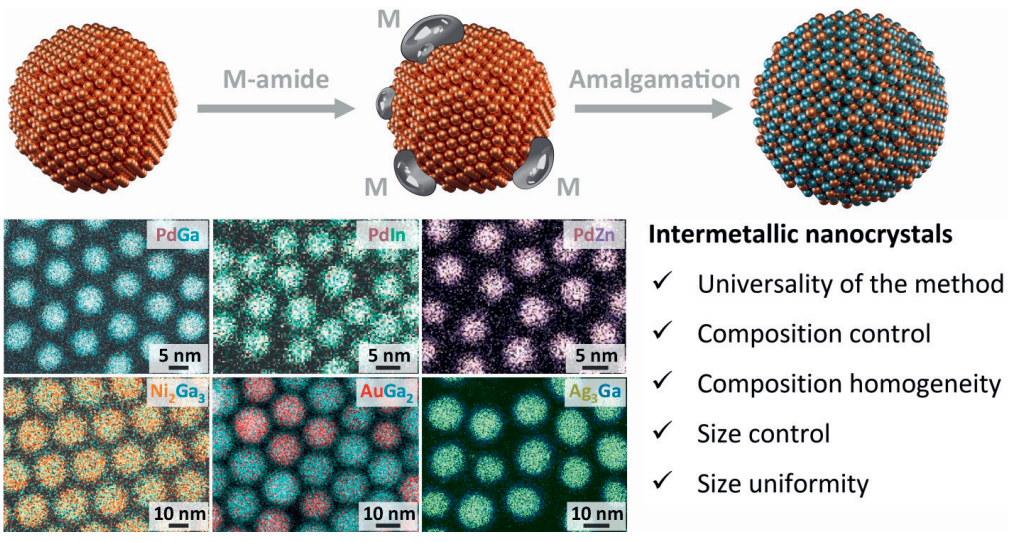

Fig. 13. Amalgamation synthesis of intermetallic nanocrystals: Schematic of the process, examples of bimetallic compositions, and structural assets enabled by our new synthetic method.[21]

powder diffractometers. The phase analysis and refinements were performed by Rietveld refinements with FULLPROF software package.[23] Start models for the structures were taken from the ICSD database or from single crystal structure analysis for the new phases.

In order to determine the quantitative and qualitative composition of phases, the analysis was performed using a scanning electron microscope with an EDS/WDS analyzer. Microstructures were observed, and phase content was measured by TESCAN Scanning Electron Microscopy (SEM). A smooth surface of the specimen was prepared using SiC papers and diamond pastes down to 1 μm grain size.

4.3 *Crystal Structure Studies*

The crystal structures were determined by single crystal X-ray diffraction methods. We are especially interested in mechanisms of forming compounds and solid solutions. We tried to obtain a single crystal from an alloy with different compositions for the following analysis on an X-ray single-crystal diffractometer. An Xcalibur diffractometer from Oxford Diffraction, equipped with a Sapphire2 CCD detector and an ENHANCE X-ray source option was used. Data analysis is performed using the SHELX program package.[24]

4.4 *Electronic Structure Calculations*

For a detailed analysis of the crystal structures, we visualized them from the refined/solved data using the DIAMOND and VESTA software packages. This allowed us to demonstrate important crystallographic information, such as the relative arrangement of atoms in the unit cells and the coordination polyhedra for each atom position and individual features for each structure. This also allowed us to identify and evaluate tetrahedral and octahedral voids in which hydrogen can potentially be stored for each phase. After the voids were identified, the chemical nature of their surroundings was also clarified.

The electronic structures of the compounds were calculated using the method of strong binding of linear muffin-tin orbitals (TB–LMTO) in the approximation of atomic spheres (TB–LMTO–ASA) using experimental crystallographic data that were obtained from single crystals. Exchange and correlation were interpreted in the local density approximation. All the figures and graphics concerning electron structure calculations were generated using wxDragon.

4.5 *Electrochemical Studies and Hydrogenation of Alloys*

Electrochemical tests to identify the best-performance anode materials for Metal-Hydride batteries were used. Electrochemical Analyzer/Workstation CH Instruments Model 600E Series, USA) and battery analyser (MTI Corporation, USA) were used. The chrono-volt-amperometric electrochemical characteristics of systems were determined by following electrochemical methods: Cyclic voltammetry (CVA), Chronopotentiometry (CP), Chronocoulometry (CC), and Electrochemical Impedance Spectroscopy (EIS). Anode materials were tested in SWAGELOK-type cells.

The hydrogen absorption and desorption measurements for Mg-Li–alloy were performed using the IMI-COR (Hiden Isochema) manometric hydrogen storage analyzer. The Sieverts method, up to a pressure of 60 bar in the temperature range from 20 °C up to 450 °C, were used. The results of the hydrogen absorption/desorption measurements were represented in P-C-T diagrams.

5. Conclusions

In this paper, we address the open challenges of H_2 storage. The focal point of research is to find hydrogen-related materials for practical use as MHHS systems and MH batteries. The substitutional alloying, compositional additives, and nanostructuring effects and their influence on the hydrogen sorption properties of intermetallic phases are discussed. Considering the Metal-Hydride Hydrogen Storage technology, $LaNi_5$ is widely used as a conventional storage material with 1.25 wt.% of H_2 capacity and the ability to perform at room temperature. There are several companies that develop products on the basis of this technology, such as Hydroxia, Hystorsys, Lavo or H2ToGo. However, the technology still waits on material discovery, which will provide a necessary boost for the H_2-enabling green and sustainable economy of the future.

The approaches proposed by us, which are based on the disordering of alloys up to a high-entropy state, modification with composite additives, and nanostructuring, are useful in the search for new hydrogen sorption materials. The correctness of these approaches is shown by the obtained experimental data given in this article.

In the outlook, studying nanoscale intermetallic nanocrystals may bring sufficient benefits for H_2 storage technology. By leveraging reduced diffusion lengths and dynamic lattice characteristics, intermetallic nanocrystals present a viable avenue to enhance the reversibility and durability of H_2 storage devices.

Acknowledgements

This research was supported by the the National Research Foundation of Ukraine (2022.01/0064).

Author Contributions

Nazar Pavlyuk: Methodology, Investigation, Data curation.
Vasyl Kordan: Methodology, Investigation, Data curation.
Grygoriy Dmytriv: Validation, Resources, Methodology, Investigation.
Maksym Yarema: Writing – review & editing, Methodology, Supervision, Conceptualization.
Volodymyr Pavlyuk: Writing – review & editing, Methodology, Investigation, Validation, Supervision, Funding acquisition, Conceptualization.

Declaration of Competing Interest

The authors declare that they have no known competing financial interests or personal relationships that could have appeared to influence the work reported in this paper.

Received: October 27, 2024

[1] N. Klopčič, I. Grimmer, F. Winkler, M. Sartory, A. Trattner. *J. Energy Stor*. **2023**, *72*, 108456. https://doi.org/10.1016/j.est.2023.108456.
[2] J. F. Herbst, M. S. Meyer, *Structural, J. Alloy Compd*. **2010**, *492*, 65, https://doi.org/10.1016/j.jallcom.2009.12.032.
[3] V. Pavlyuk, G. Dmytriv, I. Chumak, O. Gutfleisch, I. Lindemann, H. Ehrenberg, *Int. J. Hydrogen Energy* **2013**, *38*, 5724, https://doi.org/10.1016/j.ijhydene.2013.02.078.
[4] V. Pavlyuk, W.Ciesielski, N.Pavlyuk, D.Kulawik, G.Dmytriv, *Int. J. Hydrogen Energy* **2021**, *46*, 22864, https://doi.org/10.1016/j.ijhydene.2021.04.127.
[5] F. J. Desai, Md N. Uddin, M. M. Rahman, R. Asmatulu, *Int. J. Hydrogen Energy*, **2023**, *48*, 29256, https://doi.org/10.1016/j.ijhydene.2023.04.029.
[6] J.-M. Joubert, V. Paul-Boncour, F. Cuevas, J. Zhang, M. Latroche, *J. Alloy Compd*. **2021**, *862*, 158, https://doi.org/10.1016/j.jallcom.2020.158163.
[7] V. Yartys, M. Lototskyy, *J. Alloy Compd*. **2022**, *916*, 165219, https://doi.org/10.1016/j.jallcom.2022.165219.
[8] N. Pavlyuk, G. Dmytriv, V. Pavlyuk, I. Chumak, S. Indris, H. Ehrenberg, *J. Phase Equilib. Diffus*. **2022**, *43*, 458, https://doi.org/10.1007/s11669-022-00985-2
[9] N. Pavlyuk, G.Dmytriv, V.Pavlyuk, 'XV International Conference on Crystal Chemistry of Intermetallic Compounds (IMC-XV)', Lviv, September 25-27, **2023**.
[10] N. Rahulan, S. Gopalan, S. Kumaran, *Mat. Today: Proc*. **2019**, *18*, 2573, https://doi.org/10.1016/j.matpr.2019.07.115.

[11] I. Shin, E. A. Carter, *Acta Materialia* **2014**, *64*, 198, https://doi.org/10.1016/j.actamat.2013.10.030.
[12] E. Aghion, B. Bronfin, *Mat. Sci. Forum* **2000**, *350/351*, 19. https://doi.org/10.4028/www.scientific.net/MSF.350-351.19.
[13] M. Król, *Acta Physica Polonica: A* **2022**, *142*, 117, http://dx.doi.org/10.12693/APhysPolA.142.117.
[14] V. Pavlyuk, W. Ciesielski, N. Pavlyuk, D. Kulawik, G. Kowalczyk, A. Balińska, M. Szyrej, B. Rozdzynska-Kielbik, A. Folentarska, V. Kordan, *Mat. Chem. Phys*. **2019**, *223*, 503, https://doi.org/10.1016/j.matchemphys.2018.11.007.
[15] V. Pavlyuk, W. Ciesielski, N. Pavlyuk, D. Kulawik, M. Szyrej, B. Rozdzynska-Kielbik, V. Kordan, *Ionics*, **2019**, *25*, 2701, https://doi.org/10.1007/s11581-018-2743-8.
[16] V. Pavlyuk, D. Kulawik, W. Ciesielski, N. Pavlyuk, G. Dmytriv, *Acta Cryst. Sect. C-Struct. Chem*. **2018**, *74*, 360, https://doi.org/10.1107/S2053229618002851.
[17] H. E. Kissinger, *Anal. Chem.* **1957**, *29*, 1702.
[18] D. Li, F. Huang, B. Ren, S. Wang, W. Zhang, L. Zhu, *Sci. Rep*. **2024**, *14*, 905. https://doi.org/10.1038/s41598-024-51602-w
[19] X. Yang, Y. Lei, C. Wang, G. Zhu, W. Zhang, Q. Wang, *J. Alloys Compd*. **1998**, *265*, 264, https://doi.org/10.1016/S0925-8388(97)00287-9
[20] J. Vajo, F. Pinkerton, N. Stetson, *Nanotechn*. **2009**, *20*, 200201, https://doi.org/10.1088/0957-4484/20/20/200201
[21] J. Clarysse, A. Moser, O. Yarema, V. Wood, M. Yarema, *Sci. Adv*. **2021**, *7*, eabg1934, https://doi.org/10.1126/sciadv.abg1934.
[22] O. Yarema, A. Moser, C.-W. Chang, J. Clarysse, F. M. Schenk, E. Egüz, H. Vemulapalli, N. Mittal, E. Edison, Y.-H. Wu, D. A. Kuznetsov, C. R. Müller, M. Niederberger, C. M. Franck, V. Wood, M. Yarema, *Adv. Funct. Mater*. **2023**, 2309018, https://doi.org/10.1002/adfm.202309018.
[23] J.Rodriguez-Carvajal, *Physica B* **1993**, *192*, 55, https://doi.org/10.1016/0921-4526(93)90108-I.
[24] G.M. Sheldrick, SHELXL-97. University of Göttingen, Program for crystal structure refinement, **1997**.

License and Terms

The definitive version of this article is the electronic one that can be found at https://doi.org/10.2533/chimia.2024.869